

This article was downloaded by:

On: 25 January 2011

Access details: *Access Details: Free Access*

Publisher *Taylor & Francis*

Informa Ltd Registered in England and Wales Registered Number: 1072954 Registered office: Mortimer House, 37-41 Mortimer Street, London W1T 3JH, UK



## Liquid Crystals

Publication details, including instructions for authors and subscription information:

<http://www.informaworld.com/smpp/title~content=t713926090>

### New fluorinated terphenyl isothiocyanate liquid crystals

Amanda Parish<sup>a</sup>; Sebastian Gauza<sup>a</sup>; Shin-Tson Wu<sup>a</sup>; Jerzy Dziaduszek<sup>b</sup>; Roman Dabrowski<sup>b</sup>

<sup>a</sup> College of Optics and Photonics, University of Central Florida, USA <sup>b</sup> New Technology and Chemistry Department, Military University of Technology, Warsaw 00-908, Poland

**To cite this Article** Parish, Amanda , Gauza, Sebastian , Wu, Shin-Tson , Dziaduszek, Jerzy and Dabrowski, Roman(2008) 'New fluorinated terphenyl isothiocyanate liquid crystals', *Liquid Crystals*, 35: 1, 79 – 86

**To link to this Article:** DOI: 10.1080/02678290701749917

**URL:** <http://dx.doi.org/10.1080/02678290701749917>

PLEASE SCROLL DOWN FOR ARTICLE

Full terms and conditions of use: <http://www.informaworld.com/terms-and-conditions-of-access.pdf>

This article may be used for research, teaching and private study purposes. Any substantial or systematic reproduction, re-distribution, re-selling, loan or sub-licensing, systematic supply or distribution in any form to anyone is expressly forbidden.

The publisher does not give any warranty express or implied or make any representation that the contents will be complete or accurate or up to date. The accuracy of any instructions, formulae and drug doses should be independently verified with primary sources. The publisher shall not be liable for any loss, actions, claims, proceedings, demand or costs or damages whatsoever or howsoever caused arising directly or indirectly in connection with or arising out of the use of this material.

# New fluorinated terphenyl isothiocyanate liquid crystals

AMANDA PARISH†, SEBASTIAN GAUZA†, SHIN-TSON WU†\*, JERZY DZIADUSZEK‡ and ROMAN DABROWSKI‡

†College of Optics and Photonics, University of Central Florida, FL 32816, USA

‡New Technology and Chemistry Department, Military University of Technology, Warsaw 00-908, Poland

(Received 5 September 2007; accepted 16 October 2007)

High birefringence ( $\Delta n > 0.4$ ) nematic liquid crystals are particularly attractive for infrared applications because they enable a thinner cell gap to be used for achieving a fast response time. In this experiment, we evaluate the mesomorphic and physical properties of several fluorinated NCS terphenyl compounds. These compounds have  $\Delta n \sim 0.35$  in the visible spectral region and relatively low viscosity. In terms of applications, these compounds can be used as a dopant to enhance the figure-of-merit of commercial mixtures for display applications. We can also formulate high birefringence eutectic mixtures using solely NCS terphenyl compounds for near-IR laser beam steering applications.

## 1. Introduction

Continuous advancements in the field of infrared (IR) applications [1, 2], such as laser beam steering at  $\lambda = 1.55 \mu\text{m}$  (see [3]), demand the ongoing development of nematic liquid crystal (LC) materials with both high birefringence ( $\Delta n$ ) and low viscosity. Phase modulation applications require a  $2\pi$  optical phase change ( $\delta = 2\pi d \Delta n / \lambda$ , where  $d$  denotes the cell gap of the homogeneous LC cell and  $\lambda$  is the wavelength), which in turn requires the optical path length ( $d \Delta n$ ) to increase in proportion to the longer IR wavelengths. Another key performance parameter of IR applications is the response time, which is proportional to  $d^2$  and visco-elastic coefficient ( $\gamma_1 / K_{11}$ ). To meet the response time requirements, the two preferred approaches are to have low rotational viscosity ( $\gamma_1$ ) LC mixtures and to reduce the cell gap [4]. However, high birefringence and low rotational viscosity are opposing LC characteristics. A highly conjugated LC compound usually exhibits high viscosity because of its increased moment of inertia. Moreover, high-birefringence LC compounds usually possess high melting temperatures. To lower the melting temperature, many LC structures need to be developed and eutectic mixtures need to be formulated.

The most effective method of increasing birefringence is to elongate the  $\pi$ -electron conjugation of the LC compounds [5–10]. Conjugation length can be extended by either multiple bonds or unsaturated (phenyl) rings in the rigid core structure. However, the following problems are associated with highly conjugated LC

compounds: high melting temperature, increased viscosity, reduced ultraviolet (UV) stability and relatively low resistivity owing to ion trapping near the polyimide (PI) alignment interfaces [11]. The high melting temperature can be combated through the lateral fluorination of the rigid core and the use of eutectic mixtures. The increased viscosity is inherent to all highly conjugated compounds, but can be mitigated by the choice of polar group. UV stability can be improved by forming a rigid core of unsaturated rings instead of multiple bonds, as double and triple bonds are more susceptible to UV absorption [5, 12, 13]. Recently, it was shown that by using a multi-step purification process even a highly polar mixture can achieve resistivity at a level of  $10^{13} \Omega \text{cm}^{-1}$  (see [14, 15]). For the purpose of elongating molecular conjugation, common rigid cores are phenyl-tolane and terphenyl structures and common polar groups are cyano (CN) and isothiocyanato (NCS). Owing to the relatively low visco-elastic coefficients and improved photo-stability, NCS terphenyl compounds are preferable to CN terphenyl compounds or phenyl-tolane-based rigid core compounds. Although the linear structure of cyano terphenyls creates a larger dipole moment ( $\mu = 4.1 \text{ D}$ ) than NCS terphenyls ( $\mu = 3.7 \text{ D}$ ), the strong polarization of the carbon–nitrogen triple bond creates large, highly localized Huckel charges. Consequently, dimers are formed by strong molecular interactions between the nitrile groups and a significant increase in viscosity is observed. In contrast, NCS compounds do not form dimers and, therefore, rotational viscosity is significantly lower than analogous CN compounds [16]. Based on the above reasoning, several NCS terphenyl com-

\*Corresponding author.

pounds with different lateral fluorine substitutions are synthesized and studied in this paper. Molecular structures, mesomorphic properties and electro-optic properties of six multiple-fluorinated isothiocyanatoterphenyl single compounds are reported.

## 2. Experimental details

Several measurement techniques were utilized in characterizing the physical properties (including the birefringence, visco-elastic coefficient and figure-of-merit (FoM)) of single LC compounds in our laboratory. Measuring birefringence greater than 0.3 (at  $\lambda=633$  nm) required electro-optic measurements, as the extraordinary refractive index of the LC under study exceeded the upper limit ( $n_e>1.80$ ) of the Abbe refractometer used in the classic refractometric method. For the electro-optic method, homogeneous cells with cell gaps of  $5 \pm 0.30$   $\mu\text{m}$  were filled at elevated temperatures above the melting point of the LC under study. The optical setup included a linearly polarized He-Ne laser ( $\lambda=632.8$  nm) as the light source, a linear polarizer oriented at  $45^\circ$  with respect to the LC cell rubbing direction, and an analyser oriented perpendicular to the polarizer. The light transmittance was measured by a photodiode detector (New Focus Model 2031) and recorded digitally by a LabVIEW data acquisition system (DAQ, PCI 6110). Experimental driving parameters were a 1 kHz square-wave AC signal with peak-to-peak amplitude ramped from 0 to 5 V that was applied to indium-tin-oxide (ITO) electrodes coated on the inner surfaces of the LC cell. The cell substrates were coated with a thin layer of PI alignment film, deposited on top of the ITO electrodes, and buffed to induce a  $2^\circ$ – $3^\circ$  pre-tilt angle. The cell was mounted in a Linkam LTS 350 Large Area Heating/Freezing Stage controlled by a Linkam TMS94 Temperature Programmer. The phase retardation ( $\delta$ ) of the homogeneous cells was then measured using the LabVIEW system. The LC birefringence ( $\Delta n$ ) at wavelength  $\lambda$  and temperature  $T$  was obtained from the phase retardation ( $\delta$ ) measurements using the following equation [17]:

$$\delta = 2\pi d \Delta n / \lambda. \quad (1)$$

By measuring the free-relaxation (decay) time for a controlled phase change, the visco-elastic coefficient ( $\gamma_1/K_{11}$ ) was calculated according to the following equations [18]:

$$\delta(t) = \delta_0 \exp(-2t/\tau_0), \quad (2)$$

$$\tau_0 = \gamma_1 d^2 / (K_{11} \pi^2), \quad (3)$$

where  $\delta_0$  is the total phase change,  $\gamma_1$  is rotational

viscosity,  $d$  is the cell gap and  $K_{11}$  is the splay elastic constant. To compare the performance of LC mixtures, a FoM that takes the phase retardation and visco-elastic coefficient into account was defined as [19]

$$FoM = K_{11} (\Delta n)^2 / \gamma_1. \quad (4)$$

Each of the three physical properties,  $\Delta n$ ,  $\gamma_1/K_{11}$  and FoM, was known to be temperature dependent. Therefore, the heating/freezing stage was used to control the environmental conditions such that experimental data could be collected at approximately  $5^\circ\text{C}$  intervals over the entire nematic range of the LC material under study. As the single LC compounds under study have nematic phases at high temperatures (above  $100^\circ\text{C}$ ), fitting parameters are used to extrapolate the physical properties at room temperature.

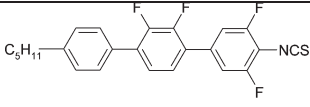
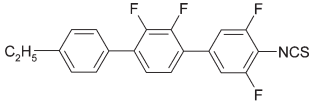
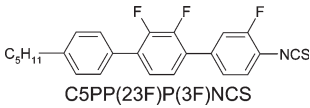
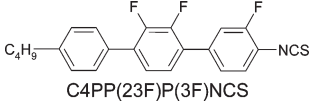
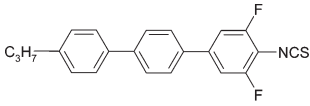
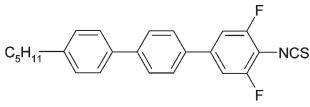
All of the thermal analyses were performed using a high-sensitivity differential scanning calorimeter (DSC; TA Instrument Model Q-100). Phase transition temperatures were measured at a scanning rate of  $2^\circ\text{C min}^{-1}$ .

## 3. Results and discussion

This experiment focused on the thermotropic, rod-like molecular systems with a polar NCS terminal group. Several variations of lateral fluorine substitutions were studied, with the goal of achieving the highest  $\Delta n$  value possible while retaining a relatively low viscosity. For this purpose, the rigid core structure of the LC compounds under study was aromatic terphenyl (benzene) rings, as the unsaturated residues are rich in  $\pi$ -electrons. These rings are particularly desirable to elongate the  $\pi$ -electron conjugation through the rod-like molecule by increasing the polarizability along the principal molecular axis. At the same time photochemical stability should not be jeopardized.

Based on previous experience [20] with highly conjugated linear molecular structures, three different configurations of laterally fluorinated terphenyl isothiocyanates were investigated, with two homologues of each structure. Table 1 lists the compound structures and their mesomorphic properties. For comparison, figure 1 illustrates phase transition temperatures with respect to the different lateral fluorine substitutions. The clearing points of the double-fluorinated structures were found to be the highest (compounds **5** and **6**). Compound **2** showed the highest melting point temperature and lowest clearing point temperature among investigated group of structures. Moreover, heat enthalpy of the melting point of compound **2** exceeded  $7 \text{ kcal mole}^{-1}$ . Such properties suggest that a two-carbon chain was too short for the long and rigid

Table 1. Compound structures and their phase transition temperatures and heat fusion enthalpy.

| ID No. | Structure   | Phase transition temperature (°C)  | $\delta H$ (Cr-N) (cal mole <sup>-1</sup> ) |
|--------|---|--|---|
| 1      | <br>C5PP(23F)P(35F)NCS | Cr 90.71 Sm(A) 137.93 N 172.98 Iso Iso 171.92N 136.4<br>Sm(A) 86.49 Cr   | 4089  |
| 2      | <br>C2PP(23F)P(35F)NCS | Cr 121.96 N 152 Iso Iso 151.1 N 103.02 Cr                                | 7040  |
| 3      | <br>C5PP(23F)P(3F)NCS  | Cr 73.17 Sm(A) 112.22 N 174.62 Iso Iso 173.38 N 109.98<br>Sm(A) 62.97 Cr | 4622  |
| 4      | <br>C4PP(23F)P(3F)NCS  | Cr 90.09 Sm(A) 104.53 N 163.32 Iso Iso 162.2 N 101.58<br>Sm(A) 79.5 Cr   | 4693  |
| 5      | <br>C3PPP(35F)NCS      | Cr 106.88 N 202.61 Iso Iso 201.0 N 100.47 Cr                             | 3359  |
|        | <br>C5PPP(35F)NCS    |  |   |

6

terphenyl molecular core to provide attractive mesomorphic properties by means of low melting point and wide temperature range of the nematic phase, even if the rigid core was fluorinated extensively. Pentyl homologues were chosen for the melting point comparison. Surprisingly, lateral substitution of four fluorines did not lower the melting point further than triple fluorination. From the point of view of the mesomorphic properties, double fluorination at the

phenyl ring with NCS terminal group was the most favourable. The melting points of the pentyl homologues with different degrees of lateral fluorination follow the order shown below:

Compound 3 < Compound 1 < Compound 6.

As is common with highly conjugated linear structures, a smectic phase was observed in four of the six compounds under study. The number of fluorine substitutions had no obvious effect on suppressing the smectic transition. However, a shorter alkyl chain did suppress the smectic phase in both the double- and tetra-fluorinated structures (compounds 2 and 5). If the smectic to nematic transition was considered, double- and triple-fluorinated compounds showed similar transition temperatures. Clearing temperature was significantly higher for the double-fluorinated compound (compound 6):

Compound 1  $\approx$  Compound 3 < Compound 6.

Shorter chain homologues of double- and triple-

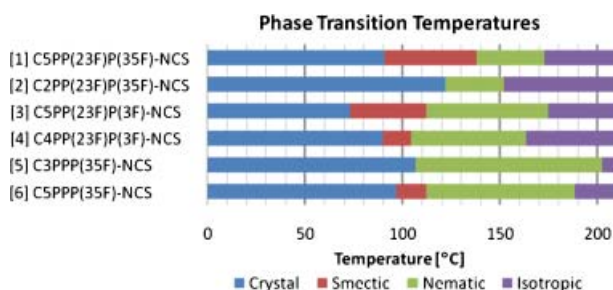


Figure 1. Phase transition temperatures comparison for the investigated structures.

fluorinated terphenyls did not show the smectic phase in the phase transitions sequence. We were not successful in obtaining less than a four-carbon chain homologue of the triple-fluorinated NCS terphenyl with sufficient chemical purity, thus data was not included in this comparison. Further synthesis must be conducted in order to specifically prove whether absence of a smectic phase was an effect of double substitution at 3',5'' positions of the phenyl ring with polar terminal group or whether the length of flexible alkyl chain was the determining factor in suppressing the smectic phase.

Melting heat enthalpy was determined using DSC analysis and found the double-fluorinated compounds to have the lowest  $\Delta H$  values ( $<3400 \text{ cal mole}^{-1}$ ), the triple-fluorinated compounds to have mid-range  $\Delta H$  values around  $4600 \text{ cal mole}^{-1}$  and the tetra-fluorinated compounds to have mid-range ( $4089 \text{ cal mole}^{-1}$  for compound **1**) and high ( $7040 \text{ cal mole}^{-1}$  for compound **2**)  $\Delta H$  values. As figure 1 illustrates, Compounds **5** and **6** are promising candidates for eutectic mixture formulation as they exhibited the best mesomorphic properties: widest nematic range, relatively low melting points, the highest clearing points, low melting heat enthalpy and no evidence of a smectic phase for compound **5**.

High birefringence ( $\Delta n$ ) values were expected for the compounds in question, as the unsaturated rings of the terphenyl structure elongate the  $\pi$ -electron conjugation through entire rigid core of the molecules. Laterally unsubstituted terphenyl compounds have been shown to exhibit very high melting points. To lower the melting point and diminish the tendency of terphenyl com-

pounds to form a smectic phase, multiple lateral fluorine substitutions were made. However, this lowers the birefringence of the compound, as laterally substituted fluorine atoms trap  $\pi$ -electrons and pull them away from the conjugation along the main molecular axis.

The experimental data and fitting results for birefringence of the six compounds are illustrated in figure 2, and show birefringence values greater than 0.36 for all structures when extrapolated to room temperature ( $25^\circ\text{C}$ ). Figure 3 illustrates the fitted curves plotted against reduced temperature ( $T/T_c$ ) in order to account for the different clearing temperature so that the structural effects can be compared. Of the three differently fluorinated systems studied, homologues C3PPP(3,5F)-NCS and C5PPP(3,5F)-NCS (compounds **5** and **6**) exhibited the largest birefringences, 0.4430 and 0.4153, respectively, when extrapolated to room temperature. This fluorination structure exhibited particularly desirable performance parameters owing to the fluorine positions being adjacent to the polar NCS group, as an electron potential is created at one end of the molecule and thereby increases the polarizability of the molecule at the microscopic scale. This, combined with high clearing point temperatures, increases the total birefringence while maintaining the suppression of the smectic phase in compound **5**. Introducing a third lateral fluorine and reconfiguring the position of the other two fluorine to 2',3',3'' positions of the terphenyl rigid core (4-alkyl-2',3',3''-trifluoro-4''-isothiocyanato-[1,1';4',1'']terphenyl; compounds **3** and **4**) decreases birefringence significantly as shown in figure 2. When

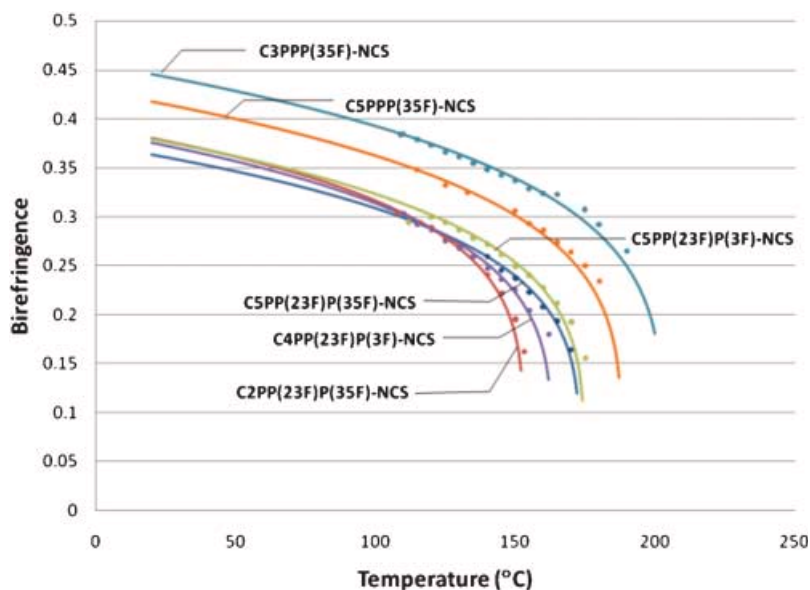


Figure 2. Temperature-dependent birefringence of the LC compounds studied.



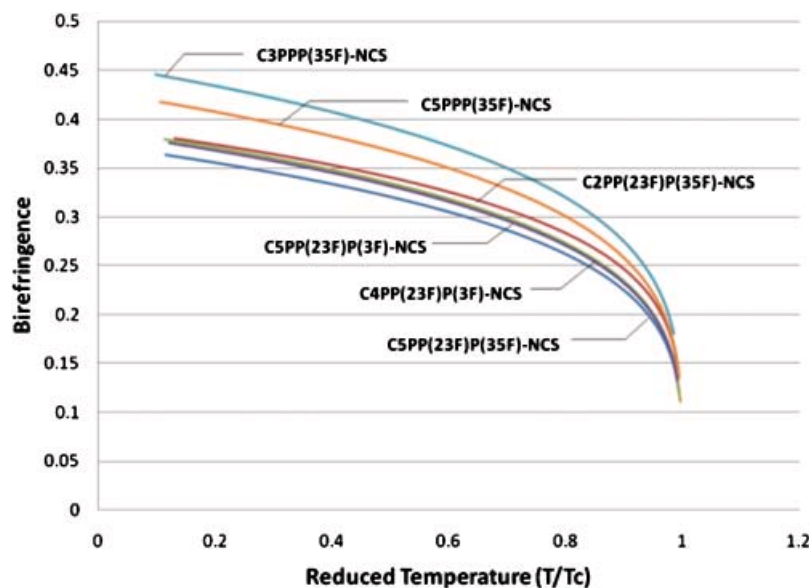


Figure 3. Birefringence versus reduced temperature.

the reduced temperature is used to offset the effect of clearing point temperature, the loss of birefringence owing to the additional third fluorine and lateral substituent reconfiguration is more evident over the entire temperature range of the nematic phase.

Among the compounds investigated, tetra-fluorinated terphenyls demonstrate the lowest birefringence with respect to the alkyl chain length, which further decreases  $\Delta n$  as the structure is elongated. The visco-elastic coefficient ( $\gamma_1/K_{11}$ ) is calculated from the free-relaxation time and characterized by the amount of time

and energy required to rotate the LC molecules. Figure 4 summarizes both experimental data and fitting results for the six compounds under study and figure 5 illustrates the fitted curves plotted against reduced temperature ( $T/T_c$ ). From figure 5, it is evident that the structures with more fluorine substitutions have higher visco-elastic coefficients over the entire nematic range. This is anticipated, as the structures with more fluorine substitutions have higher molecular weight with slightly larger cross section, and may be subjects for stronger molecular interactions with neighbouring molecules

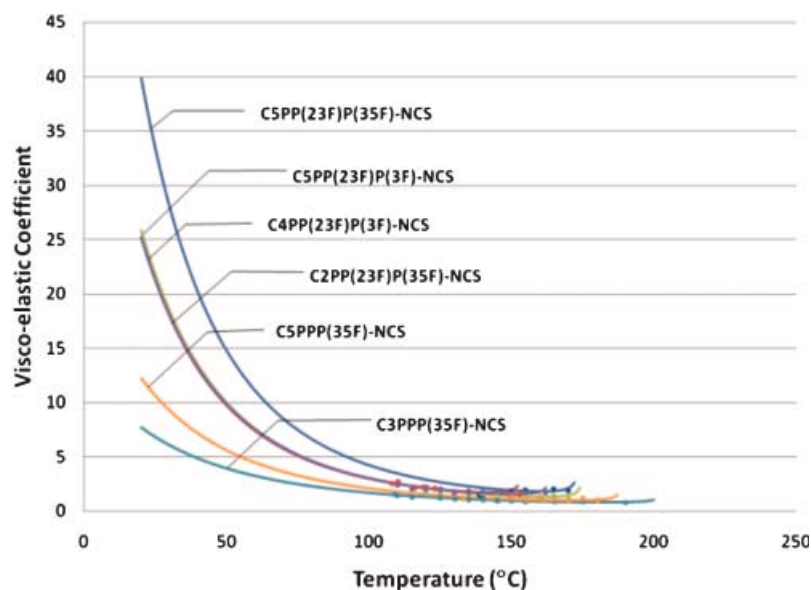


Figure 4. Temperature-dependent visco-elastic coefficient  $\gamma_1/K_{11}$  of the LC compounds studied.

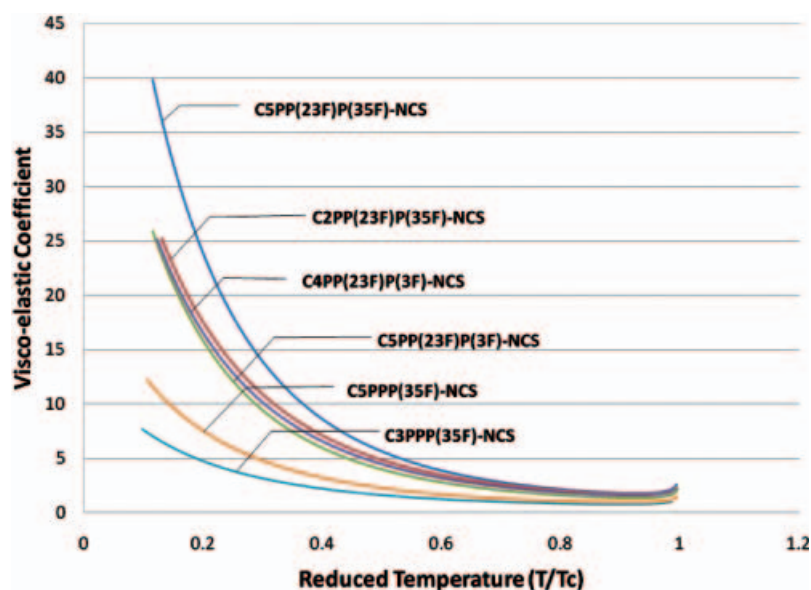


Figure 5. Temperature-dependent visco-elastic coefficient  $\gamma_1/K_{11}$  versus reduced temperature.

owing to the additional slightly negative charges on the surface. Considering all of the above, it can be surmised that additional fluorine substitutions will negatively affect the visco-elastic coefficient. This can be easily analysed on the basis of figures 4 and 5.

FoM was used for a comparison of the compound switching speed. The birefringence and visco-elastic coefficient can be compared directly, but the response time can only be compared if each compound is studied by utilizing a cell gap that exactly matches its birefringence in order to result in the best possible response time. FoM eliminates the necessity of matching the cell gap to birefringence, as the parameter is independent of the cell gap and allows side-by-side comparison of the different compounds. Moreover, because LC performance and response time are determined by several temperature-dependent factors, FoM allows the ideal operating temperature to be determined. Also, if an operating temperature is specified (e.g. room temperature), the best compound can be easily determined by the experimental data fitting according to the following equation [19]:

$$\text{FoM} = a(\Delta n)^2 \left(1 - \frac{T}{T_c}\right)^{3\beta} \exp\left(\frac{-E}{\kappa T}\right). \quad (5)$$

where  $a$  is a fitting parameter. Experimental data and appropriate fitting results of the six investigated isothiocyanatoterphenyls are summarized in figure 6 and fitted curves plotted versus reduced temperature are summarized in figure 7. It is evident that the double-fluorinated terphenyl homologues (compounds 5 and 6) are superior to triple-fluorinated or tetra-fluorinated

compounds, with almost 200% higher FoM if the C3PPP(35F)NCS compound is compared with the others at the optimum operating temperature. The fitted curves show that the ideal operating temperature is in the range of 130–160°C (FoM of 118 and 82 for compounds 5 and 6, respectively), but that even at an operating temperature of 60°C FoM values remain relatively high (55 and 35 for compounds 5 and 6, respectively). The significantly higher FoM observed in the double-fluorinated compounds is a result of both higher birefringence and lower visco-elastic coefficient values compared with the structures with more fluorine substitutions. As expected, compounds with higher numbers of laterally substituted fluorine atoms and longer terminal alkyl chain demonstrate lower FoM performance and therefore are expected to be less effective in multi-component compositions intended to reduce the response time to an applied electric field.

#### 4. Conclusion

By increasing the number of laterally substituted fluorines, we have noted that birefringence gradually decreased with a maximum of 25% loss if 4-propyl-3',5''-difluoro-4''-isothiocyanato-[1,1';4',1'']terphenyl (compound 5) was compared with 4-pentyl-2',3',3'',5''-tetrafluoro-4''-isothiocyanato-[1,1';4',1'']terphenyl (compound 1) at a temperature of 25°C. The visco-elastic coefficient was also significantly affected by increasing the number of lateral substituents. Using the same compounds for comparison (compounds 1 and 5), the  $\gamma_1/K_{11}$  coefficient showed a difference of almost 500% at 25°C. Therefore, the performance parameter, which is considered as a FoM, was substantially different for

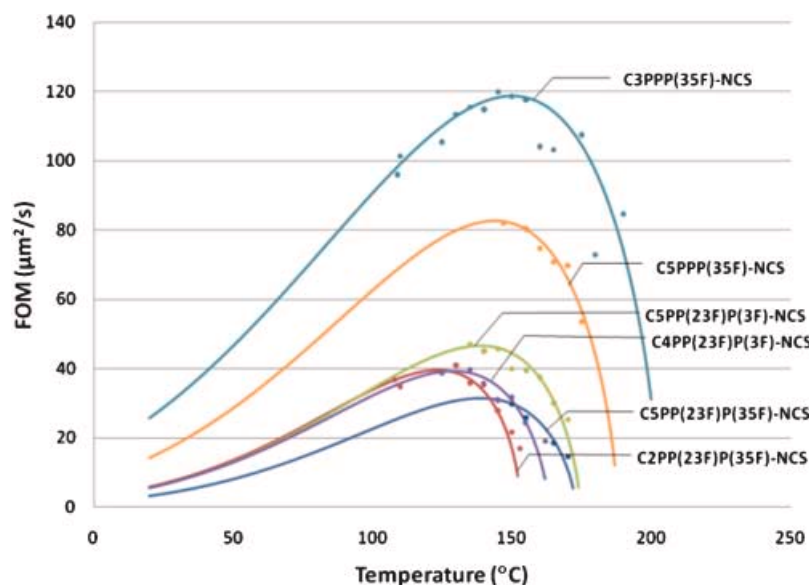


Figure 6. Temperature-dependent FoM of the LC compounds studied.

compounds presented. Detailed DSC analysis does not show a significantly lower melting point when the number of fluorine substitutions was increased from two to four. These results led to the conclusion that for the case of a rigid terphenyl-NCS core, further fluorination does not affect the mesomorphic properties to the same extent as fluorine substitutions in the positions closest to the polar group. The double-fluorinated NCS terphenyl structure showed the best overall performance of the three fluorinated structures studied. These two compounds will yield faster response times, as the higher birefringence value will allow for a thinner cell gap and

the lower viscosity will allow the molecules to be rotated faster. The mesomorphic properties (wide nematic range, suppressed smectic phase) and relatively low melting heat enthalpy makes the double-fluorinated NCS terphenyl structure an ideal candidate for eutectic mixtures and potentially an all-isothiocyanatoterphenyl-based mixture.

#### Acknowledgements

This work is supported by DARPA Bio-Optics Synthetic Systems program under Contract No. W911NF04C0048 and NATO Programme

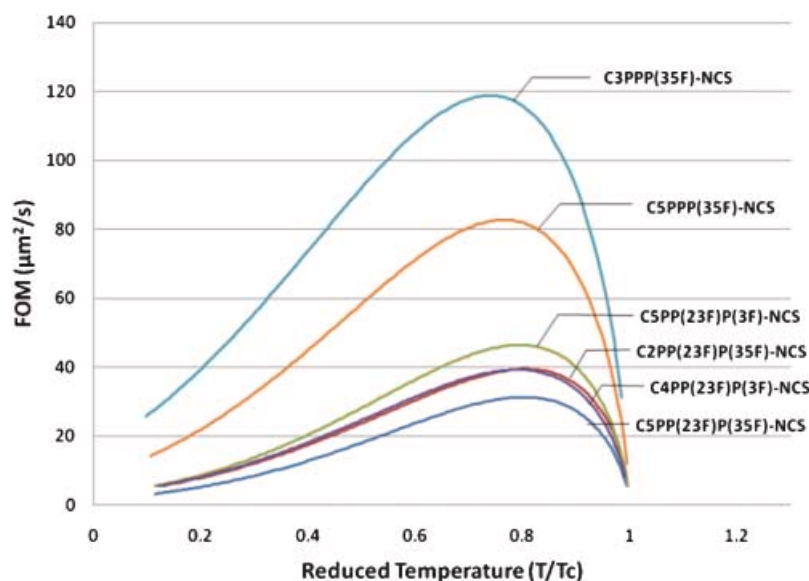


Figure 7. FOM versus reduced temperature.



Security Through Science, Collaborative Linkage Grant No. CBP.EAP.CLG 981323.

## References

- [1] U. Efron, S.T. Wu, J. Grinberg, L.D. Hess. *Opt. Eng.*, **24**, 111 (1985).
- [2] S.T. Wu. *Opt. Eng.*, **26**, 120 (1987).
- [3] P.F. McManamon, T.A. Dorschner, D.L. Corkum, L. Friedman, D.S. Hobbs, M. Holz, S. Liberman, H.Q. Nguyen, D.P. Resler, R.C. Sharp, E.A. Watson. *Proc. IEEE*, **84**, 268 (1996).
- [4] S.T. Wu, U. Efron. *Appl. Phys. Lett.*, **48**, 624 (1986).
- [5] S.T. Wu, J.D. Margerum, H.B. Meng, L.R. Dalton, C.S. Hsu, S.H. Lung. *Appl. Phys. Lett.*, **61**, 630 (1992).
- [6] S.T. Wu, C.S. Hsu, K.F. Shyu. *Appl. Phys. Lett.*, **74**, 344 (1999).
- [7] C. Sekine, K. Fujisawa, K. Iwakura, M. Minai. *Mol. Cryst. Liq. Cryst.*, **364**, 711 (2000).
- [8] S. Gauza, C.H. Wen, S.T. Wu, N. Janarthanan, C.S. Hsu. *Jpn. J. Appl. Phys.*, **43**, 7634 (2004).
- [9] S. Gauza, H. Wang, C.H. Wen, S.T. Wu, A. Seed, R. Dabrowski. *Jpn. J. Appl. Phys.*, **42**, 3463 (2003).
- [10] C.O. Catanescu, L.C. Chien. *Liq. Cryst.*, **33**, 115 (2006).
- [11] A. Spadlo, R. Dabrowski, M. Filipowicz, Z. Stolarz, J. Przedmojski, S. Gauza, Y.H. Fan, S.T. Wu. *Liq. Cryst.*, **30**, 191 (2003).
- [12] P.T. Lin, S.T. Wu, C.Y. Chang, C.S. Hsu. *Mol. Cryst. Liq. Cryst.*, **411**, 243 (2004).
- [13] S.T. Wu, U. Finkenzeller, V. Reiffenrath. *J. Appl. Phys.*, **65**, 4372 (1989).
- [14] S. Gauza, C.H. Wen, B.J. Tan, S.T. Wu. *Jpn. J. Appl. Phys.*, **43**, 7176 (2004).
- [15] I.K. Huh, Y.B. Kim. *Jpn. J. Appl. Phys.*, **41**, 6466 (2002).
- [16] J.A. Malecki, J. Nowak. *J. Mol. Liq.*, **81**, 245 (1999).
- [17] S.T. Wu, U. Efron, L.D. Hess. *Appl. Opt.*, **23**, 3911 (1984).
- [18] S.T. Wu, C.S. Wu. *Phys. Rev. A*, **42**, 2219 (1990).
- [19] S.T. Wu, A.M. Lackner, U. Efron. *Appl. Opt.*, **26**, 3441 (1987).
- [20] S. Gauza, J. Li, S.T. Wu, A. Spadlo, R. Dabrowski, Y.N. Tzeng, K.L. Cheng. *Liq. Cryst.*, **32**, 1077 (2005).